Int. J. Heat Mass Transfer. Vol. 34, No. 3, pp. 863–874, 1991
Printed in Great Britain

0017-9310/91 \$3.00+0.00

Thermal performance of split-flow heat exchangers

B. SPANG, Y. XUAN and W. ROETZEL

Institute of Thermodynamics, University of the Federal Armed Forces, Holstenhofweg 85, D-2000 Hamburg 70, F.R.G.

(*Received* 1 *December* 1989)

Abstract—Thermal analysis is carried out for split-flow heat exchangers with an even number of tube passes, arbitrary entrance and exit locations of the shellside flow, arbitrary division of the shellside fluid and variable *NTU*. A closed form solution is presented for calculating the temperature at a given position and the thermal effectiveness. The thermal performance of the split-flow exchanger is compared with that of the conventional shell and tube exchanger. The shellside pressure drop and the optimum entrance and exit locations of the shellside flow in the split-flow exchanger are discussed.

1. INTRODUCTION

SPLIT-flow heat exchangers, designated as G-type in the TEMA Standards [1], find extensive application in industry because of their heat transfer and pressure drop characteristics superior to conventional shell and tube heat exchangers. Schindler and Bates [2] discussed these merits of the split-flow exchanger and presented the relationships among the thermal effectiveness, *NTU* and the thermal flow rate ratio R for two tube pass and one shell pass exchangers. Governing equations for heat transfer in a split-flow exchanger with four tube passes were derived by Singh and Holtz [3], who made a comparison of the thermal performance between two tube pass and four tube pass split-flow exchangers [4]. Murty carried out analysis about heat transfer characteristics of one and two tube pass exchangers with the split-flow pattern on the shellside in another arrangement [5]. In all these papers, such presumptions as constant *NTU* through the whole exchanger, the even division of the shellside flow and the middle entrance location of the shellside fluid were used. Also, these results were limited to the especially given number of tube passes, respectively.

The purposes of this paper are to present governing equations for N tube passes and one shell pass (referred to as $1-N$) split-flow exchangers and formulas for calculating temperatures at a given location, the thermal effectiveness and the mean temperature difference correction factor with arbitrary divisions and variable entrance and exit locations of the shellside flow as well as piecewise change of the overall heat transfer coefficient. The influence of the division of the shellside fluid upon the pressure loss and the optimum entrance and exit locations will be discussed. The system of equations will be solved by means of matrix expression.

2. FORMULATION

In split-flow exchangers, the whole heat transfer area is divided into four subregions by a longitudinal baffle, as shown in Fig. 1. Obviously, temperatures in each subregion are governed by separate equations. To develop a general coordinate system, the origin is always set at the location where the tubeside fluid enters the heat exchanger. The following dimensionless variables and parameters are introduced to facilitate the analysis:

dimensionless flow path coordinate

$$x = \frac{1}{L} = \frac{a_i}{A_i} = \frac{a}{A};$$

dimensionless temperatures

$$t = \frac{\theta_2 - \theta_2'}{\theta_1' - \theta_2'}, \quad T = \frac{\theta_1 - \theta_2'}{\theta_1' - \theta_2'};$$

thermal flow rate ratio

$$R_1 = \frac{\dot{W}_1}{\dot{W}_2}, \quad R_2 = \frac{\dot{W}_2}{\dot{W}_1};$$

division ratio of the shellside fluid

$$\beta_a = \frac{\dot{W}_a}{\dot{W}_1}, \quad \beta_c = \frac{\dot{W}_c}{\dot{W}_1};$$

number of transfer units

$$NTU_1 = \frac{UA}{\dot{W}_1}, \quad NTU_2 = \frac{UA}{\dot{W}_2};$$

dimensionless temperature change

$$P_1 = \frac{\theta_1' - \theta_1''}{\theta_1' - \theta_2'}, \quad P_2 = \frac{\theta_2'' - \theta_2'}{\theta_1' - \theta_2'};$$

NTU ratio for tube pass i

$$\varepsilon_i = \frac{(UA)_i}{UA} = \frac{(NTU_2)_i}{NTU_2}.$$

According to the definition of the above dimensionless parameters, the following relationships occur:

NOMENCLATURE

- a heat transfer surface area along the flow path [m^2]
- A total heat transfer surface area of the exchanger [m^2]
- $\mathbf{A}, \mathbf{B}, \mathbf{C}, \mathbf{D}$ coefficient matrices
- c_h, c_h^* coefficients
- D equivalent transverse diameter of the shellside flow tunnel [m]
- d equivalent transverse diameter defined by equation (48) [m]
- E_i, F_i, G_i, H_i eigenvectors
- F mean temperature difference correction factor
- e_j, f_j, g_j, h_j constant coefficients to be determined
- $\mathbf{I}$ unit matrix
- l flow location of fluid [m]
- L length of tubes [m]
- m number of tube passes above the longitudinal baffle
- n number of tube passes below the longitudinal baffle
- N total number of tube passes, $m+n$
- NTU number of transfer units
- $O(x)$ function defined by equation (31)
- $p_1, \ldots, p_k$ vectors defined by equation (32)
- P dimensionless temperature change through the exchanger
- ΔP pressure drop [N m^{-2}]
- $\mathbf{Q}$ coefficient matrix defined by equation (34)
- b, r, s, u coefficients
- R ratio of thermal flow rates
- S coefficient vector defined by equation (34)
- $t_{i,i+1}$ intermediate temperature of the tubeside fluid
- Δt_m true mean temperature difference
- Δt_{log} logarithmic mean temperature difference
- t dimensionless temperature of the tubeside fluid
- T dimensionless temperature of the shellside fluid
- $\mathbf{T}$ dimensionless temperature vector
- U overall heat transfer coefficient [W m^{-2} K^{-1}]
- $\dot{W}$ thermal flow rate [W K^{-1}]
- x dimensionless coordinate
- $Y_1, \ldots, Y_k$ functions defined by equation (33)
- Z coefficient vector defined by equation (34).

Greek symbols
- α constant coefficient
- β division ratio of the shellside fluid
- ε_i ratio of $(NTU_2)_i$ in tube pass i to the total NTU_2 of the exchanger
- θ temperature [K]
- λ eigenvalue
- ρ_1, ρ_2 constant coefficients
- σ constant coefficient
- ω velocity of the shellside fluid [m s^{-1}].

Subscripts
- a, b, c, d subregions a, b, c and d, respectively
- 1, s shellside
- 2 tubeside
- j, k order number of elements of matrices.

Superscripts
- $'$ inlet
- $''$ outlet
- $*$ conventional shell and tube exchanger.

$$\sum_{i=1}^{N} \varepsilon_i = 1 \qquad (1)$$

because of

$$UA = \sum_{i=1}^{N} (UA)_i \qquad (2)$$

and $\beta_a + \beta_c = 1$ as well as

$$\frac{P_1}{P_2} = \frac{NTU_1}{NTU_2} = R_2 = \frac{1}{R_1}. \qquad (3)$$

In the analysis the major assumptions are made as follows:

(1) The shellside fluid is completely mixed at any cross-section of its nominal flow path and no by-passing occurs.

(2) Piecewise constant heat transfer coefficient: the heat transfer coefficient is assumed to be constant in a pass in each subregion, but it may vary with passes and subregions.

(3) There is no phase change and heat losses are negligible.

(4) Specific heat capacities are constant throughout the exchanger.

The whole heat exchange region is divided into subregions a, b, c and d. The corresponding temperatures of the fluids are marked as T_a, t_a, T_b, t_b, T_c, t_c, T_d and t_d, respectively. By means of the above dimensionless variables and parameters, the governing equations can be derived for each subregion. For subregion a, the energy balance yields

$$UA\varepsilon_i(T_a - t_{ai}) = \pm(-1)^i \dot{W}_2 \frac{dt_{ai}}{dx} \quad (i = 1, 2, \ldots, m) \qquad (4)$$

$$-\dot{W}_a \frac{dT_a}{dx} = \sum_{i=1}^{m} \pm(-1)^i \dot{W}_2 \frac{dt_{ai}}{dx}. \tag{5}$$

These two equations can be reformed as

$$\frac{dt_{ai}}{dx} = \pm(-1)^i \varepsilon_i NTU_2(T_a - t_{ai}) \quad (i = 1, 2, \ldots, m) \tag{6}$$

$$\frac{dT_a}{dx} = \frac{NTU_1}{\beta_a} \sum_{i=1}^{m} \varepsilon_i t_{ai} - \frac{NTU_1}{\beta_a} T_a \sum_{i=1}^{m} \varepsilon_i. \tag{7}$$

Noting $\dot{W}_b = \dot{W}_a$, one can also obtain equations pertinent to subregion b

$$\frac{dt_{bi}}{dx} = \pm(-1)^i \varepsilon_i NTU_2(T_b - t_{bi})$$

$$(i = m+1, m+2, \ldots, N) \tag{8}$$

$$\frac{dT_b}{dx} = -\frac{NTU_1}{\beta_a} \sum_{i=m+1}^{N} \varepsilon_i t_{bi} + \frac{NTU_1}{\beta_a} T_b \sum_{i=m+1}^{N} \varepsilon_i. \tag{9}$$

Similarly, in subregion c the governing equations are

$$\frac{dt_{ci}}{dx} = \pm(-1)^i \varepsilon_i NTU_2(T_c - t_{ci}) \quad (i = 1, 2, \ldots, m) \tag{10}$$

$$\frac{dT_c}{dx} = -\frac{NTU_1}{\beta_c} \sum_{i=1}^{m} \varepsilon_i t_{ci} + \frac{NTU_1}{\beta_c} T_c \sum_{i=1}^{m} \varepsilon_i. \tag{11}$$

In subregion d there are the following equations:

$$\frac{dt_{di}}{dx} = \pm(-1)^i \varepsilon_i NTU_2(T_d - t_{di})$$

$$(i = m+1, m+2, \ldots, N) \tag{12}$$

$$\frac{dT_d}{dx} = \frac{NTU_1}{\beta_c} \sum_{i=m+1}^{N} \varepsilon_i t_{di} - \frac{NTU_1}{\beta_c} T_d \sum_{i=m+1}^{N} \varepsilon_i \tag{13}$$

where the positive sign (+) and the negative sign (−) of the sign (±) in the above-mentioned equations are valid for tube flow pattern I and tube flow pattern II, respectively, which are shown in Fig. 1.

Obviously, there are $(2N+4)$ ordinary linear differential equations with constant coefficients. These

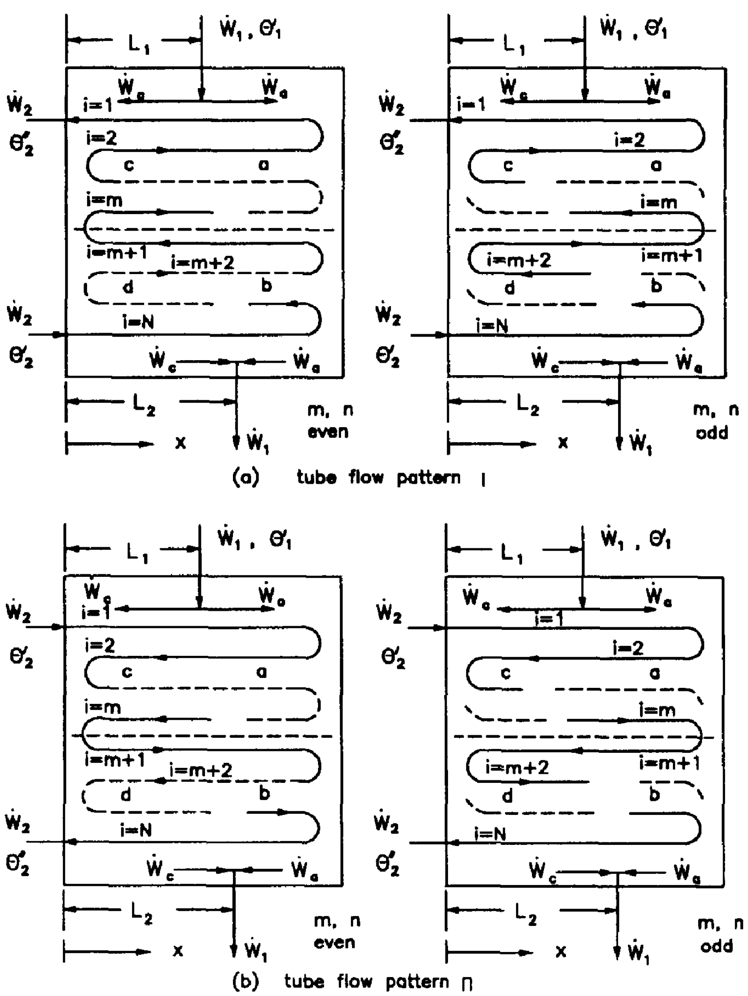

FIG. 1. Thermal scheme of $1-N$ split-flow heat exchanger.

Table 1. Boundary conditions for $t(x)$

	$x=0$	$x=1$	Tube flow pattern I	Tube flow pattern II
m,n even	$t_{ci}=t_{ci+1}=t_{ci,i+1}$ $i=2,4,\ldots,m-2$	$t_{ai}=t_{ai+1}=t_{ai,i+1}$ $i=1,3,\ldots,m-1$	$t_{dN}(0)=0$	$t_{c1}(0)=0$
	$t_{di}=t_{di+1}=t_{di,i+1}$ $i=m+2,m+4,\ldots,N-2$	$t_{bi}=t_{bi+1}=t_{bi,i+1}$ $i=m+1,m+3,\ldots,N-1$		
m,n odd	$t_{ci}=t_{ci+1}=t_{ci,i+1}$ $i=2,4,\ldots,m-1$	$t_{ai}=t_{ai+1}=t_{ai,i+1}$ $i=1,3,\ldots,m-2$	$t_{dN}(0)=0$	$t_{c1}(0)=0$
	$t_{di}=t_{di+1}=t_{di,i+1}$ $i=m+1,m+3,\ldots,N-2$	$t_{bi}=t_{bi+1}=t_{bi,i+1}$ $i=m+2,m+4,\ldots,N-1$		

Table 2. Interface conditions for $t(x)$

$x=x_1=L_1/L$	$x=x_2=L_2/L$	m,n even	m,n odd
$t_{ai}=t_{ci}$ $i=1,2,\ldots,m$	$t_{bi}=t_{di}$ $i=m+1,m+2,\ldots,N$	$t_{cm}(0)=t_{dm+1}(0)$	$t_{am}(1)=t_{bm+1}(1)$

equations are a conjugal system through interface conditions. To solve this system of differential equations $(2N+4)$ determinant conditions are necessary. Tables 1–3 give the related $(2N+4)$ conditions.

In principle, the solution of these $(2N+4)$ differential equations with such $(2N+4)$ determinant conditions is very tedious. Fortunately, all equations are homogeneous and we can readily solve this system of equations by means of linear algebra [6]. The matrix notation is introduced to express the system briefly. For subregion a, equations (6) and (7) can be written as

$$\frac{d\mathbf{T}_A}{dx}=\mathbf{AT}_A \tag{14}$$

where $\mathbf{T}_A=(t_{a1},t_{a2},\ldots,t_{am},T_a)^T$ and $\mathbf{A}$ is a constant coefficient matrix with order $(m+1)$, the elements of which are given as follows:

$$a_{ij}=\begin{cases}0 & i\neq j \quad i,j=1,2,\ldots,m\\ \pm(-1)^{i+1}\varepsilon_i NTU_2 & i=j \quad i,j=1,2,\ldots,m\\ \pm(-1)^{i}\varepsilon_i NTU_2 & j=m+1 \quad i=1,2,\ldots,m\end{cases}$$

$$a_{ij}=\begin{cases}\dfrac{NTU_1}{\beta_a}\varepsilon_j & j=1,2,\ldots,m\\ -\dfrac{NTU_1}{\beta_a}\displaystyle\sum_{k=1}^{m}\varepsilon_k & j=m+1\end{cases} \quad i=m+1.$$

Similarly, for subregion b

$$\frac{d\mathbf{T}_B}{dx}=\mathbf{BT}_B \tag{15}$$

where $\mathbf{T}_B=(t_{bm+1},t_{bm+2},\ldots,t_{bN},T_b)^T$ and $\mathbf{B}$ is a constant coefficient matrix with order $(n+1)$, the elements of which are given as follows:

$$b_{ij}=\begin{cases}0 \quad i\neq j\\ \qquad i,j=m+1,m+2,\ldots,N\\ \pm(-1)^{i+1}\varepsilon_i NTU_2 \quad i=j\\ \qquad i,j=m+1,m+2,\ldots,N\\ \pm(-1)^{i}\varepsilon_i NTU_2 \quad j=N+1\\ \qquad i=m+1,m+2,\ldots,N\end{cases}$$

$$b_{ij}=$$

$$\begin{cases}-\dfrac{NTU_1}{\beta_a}\varepsilon_j & j=m+1,m+2,\ldots,N\\ \dfrac{NTU_1}{\beta_a}\displaystyle\sum_{k=m+1}^{N}\varepsilon_k & j=N+1\end{cases} \quad i=N+1.$$

For subregion c

$$\frac{d\mathbf{T}_C}{dx}=\mathbf{CT}_C \tag{16}$$

where $\mathbf{T}_C=(t_{c1},t_{c2},\ldots,t_{cm},T_c)^T$ and $\mathbf{C}$ is a constant coefficient matrix with order $(m+1)$, the elements of which are given as follows:

$$c_{ij}=\begin{cases}0 & i\neq j \quad i,j=1,2,\ldots,m\\ \pm(-1)^{i+1}\varepsilon_i NTU_2 & i=j \quad i,j=1,2,\ldots,m\\ \pm(-1)^{i}\varepsilon_i NTU_2 & j=m+1 \quad i=1,2,\ldots,m\end{cases}$$

Table 3. Boundary and interface conditions for $T(x)$

$x=0$	$x=x_1=L_1/L$	$x=1$
$T_c=T_d$	$T_c=1.0,\ T_a=1.0$	$T_a=T_b$

$$c_{ij} = \begin{cases} -\dfrac{NTU_1}{\beta_c}\varepsilon_j & j = 1,2,\ldots,m \\ \dfrac{NTU_1}{\beta_c}\sum_{k=1}^{m}\varepsilon_k & j = m+1 \end{cases} \quad i = m+1.$$

For subregion d

$$\frac{d\mathbf{T}_D}{dx} = \mathbf{D}\mathbf{T}_D \tag{17}$$

where $\mathbf{T}_D = (t_{dm+1}, t_{dm+2}, \ldots, t_{dN}, T_d)^T$ and $\mathbf{D}$ is a constant coefficient matrix with order $(n+1)$, the elements of which are given as follows:

$$d_{ij} = \begin{cases} 0 \quad i \neq j \\ \qquad i,j = m+1, m+2, \ldots, N \\ \pm(-1)^{i+1}\varepsilon_i NTU_2 \quad i = j \\ \qquad i,j = m+1, m+2, \ldots, N \\ \pm(-1)^{i}\varepsilon_i NTU_2 \quad j = N+1 \\ \qquad i = m+1, m+2, \ldots, N \end{cases}$$

$$d_{ij} = \begin{cases} \dfrac{NTU_1}{\beta_c}\varepsilon_j & j = m+1, m+2, \ldots, N \\ -\dfrac{NTU_1}{\beta_c}\sum_{k=m+1}^{N}\varepsilon_k & j = N+1 \end{cases}$$
$$i = N+1. \tag{18}$$

Now we will search a general solution matrix for each subregion by means of eigenvalues and eigenvectors. Assuming E exp $(\lambda_a x)$ to be a solution of subsystem (14), one can obtain

$$\lambda_a E \exp(\lambda_a x) = \mathbf{A}E \exp(\lambda_a x). \tag{19}$$

Since $\exp(\lambda_a x) \neq 0$, so that

$$(\mathbf{A} - \lambda_a \mathbf{I})E = 0. \tag{20}$$

In order to obtain a non-zero solution for vector E, there must be

$$\det(\mathbf{A} - \lambda_a \mathbf{I}) = 0. \tag{21}$$

This is a polynomial equation of degree $(m+1)$ in λ_a, and hence there are $(m+1)$ roots λ_{ai} ($i = 1, 2, \ldots, m+1$), which are called eigenvalues of $\mathbf{A}$, and the corresponding E_i ($i = 1, 2, \ldots, m+1$) are called eigenvectors of $\mathbf{A}$

$$E_i = (e_{1i}, e_{2i}, \ldots, e_{m+1,i})^T. \tag{22}$$

Similarly, for subsystem (15) there are $(n+1)$ eigenvalues λ_{bi} and corresponding eigenvectors F_i ($i = m+1, m+2, \ldots, N+1$)

$$F_i = (f_{m+1,i}, f_{m+2,i}, \ldots, f_{N+1,i})^T. \tag{23}$$

For subsystem (16) there are $(m+1)$ eigenvalues λ_{ci} as well as eigenvectors G_i ($i = 1, 2, \ldots, m+1$)

$$G_i = (g_{1i}, g_{2i}, \ldots, g_{m+1,i})^T. \tag{24}$$

Finally, derivation of subsystem (17) gives $(n+1)$ eigenvalues λ_{di} and corresponding eigenvectors H_i ($i = m+1, m+2, \ldots, N+1$)

$$H_i = (h_{m+1,i}, h_{m+2,i}, \ldots, h_{N+1,i})^T. \tag{25}$$

If all these eigenvalues are distinct in each subsystem, respectively, temperature vectors to be determined can be expressed as

$$\mathbf{T}_A = \sum_{j=1}^{m+1} e_j E_j \exp(\lambda_{aj} x) \tag{26}$$

$$\mathbf{T}_B = \sum_{j=m+1}^{N+1} f_j F_j \exp(\lambda_{bj} x) \tag{27}$$

$$\mathbf{T}_C = \sum_{j=1}^{m+1} g_j G_j \exp(\lambda_{cj} x) \tag{28}$$

$$\mathbf{T}_D = \sum_{j=m+1}^{N+1} h_j H_j \exp(\lambda_{dj} x). \tag{29}$$

The combination of equations (26)–(29) constructs a general solution for the $1-N$ split-flow heat exchanger. However, it must be emphasized that equations (26)–(29) may fail if there occur multiple eigenvalues. In this case, these equations must be corrected. If there is an eigenvalue λ_{ai} of multiplicity k in subsystem (14), for example, a solution of the following form is suggested [7]:

$$Y = O(x)\exp(\lambda_{ai} x) \tag{30}$$

where $O(x)$ is a polynomial of degree k, given by

$$O(x) = p_1 + p_2 x + p_3 x^2 + \cdots + p_k x^{k-1}. \tag{31}$$

Insertion of equation (31) in subsystem (14) yields

$$(\mathbf{A} - \lambda_{ai}\mathbf{I})(p_1 + p_2 x + p_3 x^2 + \cdots + p_k x^{k-1}) = p_2 + 2p_3 x + \cdots + (k-1)p_k x^{k-2}.$$

In order for this equation to be valid for all x, we equate coefficients of x and obtain

$$\begin{aligned} (\mathbf{A} - \lambda_{ai}\mathbf{I})p_k &= 0 \\ (\mathbf{A} - \lambda_{ai}\mathbf{I})p_{k-1} &= (k-1)p_k \\ (\mathbf{A} - \lambda_{ai}\mathbf{I})p_{k-2} &= (k-2)p_{k-1} \\ &\vdots \\ (\mathbf{A} - \lambda_{ai}\mathbf{I})p_1 &= p_2. \end{aligned} \tag{32}$$

Since $\det(\mathbf{A} - \lambda_{ai}\mathbf{I}) = 0$, the remaining non-homogeneous system can be solved, provided that the rank of $(\mathbf{A} - \lambda_{ai}\mathbf{I})$ is equal to the rank of the augmented matrix formed by $(\mathbf{A} - \lambda_{ai}\mathbf{I})$ with non-homogeneous terms in equation (32). From a set of vectors $[\![p_1, p_2, \ldots, p_k]\!]$, the following solutions can be constructed:

$$\begin{aligned} Y_1 &= p_1 \exp(\lambda_{ai} x) \\ Y_2 &= (p_1 + p_2 x)\exp(\lambda_{ai} x) \\ &\vdots \\ Y_k &= (p_1 + p_2 x + \cdots + p_k x^{k-1})\exp(\lambda_{ai} x) \end{aligned} \tag{33}$$

which are also solutions of subsystem (14). With the solutions related to other distinct eigenvalues

λ_{aj}, a general solution for subsystem (14) can be constructed by a linear superposition. To do this, E_j ($j = i, i+1, \ldots, i+k$) in equation (26) will be replaced by Y_j ($j = 1, 2, \ldots, k$), respectively. In this way one can readily solve the problem with multiple eigenvalues. In the following analysis we will concentrate on the case where all eigenvalues are different. The procedure for the case with multiple eigenvalues is similar.

The $(2N+4)$ constant coefficients e_j, f_j, g_j and h_j in equations (26)–(29) must be determined according to the given boundary and interface conditions in order to find the particular solution for the original problem. Regarding the conditions in Tables 1–3, a matrix equation for determining these coefficients can be written as

$$\mathbf{QZ} = \mathbf{S} \tag{34}$$

where $\mathbf{Z}$, $\mathbf{S}$ are vectors with $(2N+4)$ elements

$$\mathbf{Z} = (e_1, e_2, \ldots, e_{m+1}, f_{m+1}, f_{m+2}, \ldots, f_{N+1}, g_1, g_2, \ldots, g_{m+1}, h_{m+1}, h_{m+2}, \ldots, h_{N+1})^{\mathrm{T}}$$

$$\mathbf{S} = (0, 0, \ldots, 0, 1.0, 1.0)^{\mathrm{T}}$$

if the inlet boundary conditions for the shellside fluid at $x = x_1$ are taken as the last two equations.

Matrix $\mathbf{Q}$ of order $(2N+4)$ has elements which depend on factors, such as the multiplicity of eigenvalues, the tubeside flow pattern, the number of tube passes and the entrance and exit locations of the shellside flow. If all eigenvalues are distinct (generally, it is so), m and n are even numbers and the tubeside flow pattern is the same as that shown in Fig. 1(a), elements q_{ij} can be described as

$$q_{kj} = \begin{cases} (e_{kk,j} - e_{kk+1,j}) \exp(\lambda_{aj}) & 1 \leqslant j \leqslant m+1 \\ 0 & m+2 \leqslant j \leqslant 2N+4 \end{cases}$$

$$k = 1, 2, \ldots, m/2$$

where $kk = 2k-1$

$$q_{kj} = \begin{cases} (f_{kk,jj} - f_{kk+1,jj}) \exp(\lambda_{bjj}) & m+2 \leqslant j \leqslant N+2 \\ 0 & \text{other } j \end{cases}$$

$$k = \frac{m}{2}+1, \frac{m}{2}+2, \ldots, \frac{N}{2}$$

where $kk = 2k-1$ and $jj = j-1$

$$q_{kj} = \begin{cases} g_{kk,jj} - g_{kk+1,jj} & N+3 \leqslant j \leqslant N+m+3 \\ 0 & \text{other } j \end{cases}$$

$$k = \frac{N}{2}+1, \frac{N}{2}+2, \ldots, \frac{N+m}{2}-1$$

where $kk = 2k-N$ and $jj = j-N+2$

$$q_{kj} = \begin{cases} h_{kk,jj} - h_{kk+1,jj} & N+m+4 \leqslant j \leqslant 2N+4 \\ 0 & \text{other } j \end{cases}$$

$$k = \frac{N+m}{2}, \frac{N+m}{2}+1, \ldots, N-2$$

where $kk = 2k+2-N$ and $jj = j-N-3$

$$q_{kj} = \begin{cases} e_{kk,j} \exp(\lambda_{aj} x_1) & 1 \leqslant j \leqslant m+1 \\ -g_{kk,jj} \exp(\lambda_{cjj} x_1) & N+3 \leqslant j \leqslant N+m+3 \\ 0 & \text{other } j \end{cases}$$

$$k = N-1, N, \ldots, N+m-2$$

where $kk = k-N+2$ and $jj = j-N-2$

$$q_{kj} = \begin{cases} f_{kk,j-1} \exp(\lambda_{bj-1} x_1) & m+2 \leqslant j \leqslant N+2 \\ -h_{kk,jj} \exp(\lambda_{djj} x_1) & N+m+4 \leqslant j \leqslant 2N+4 \\ 0 & \text{other } j \end{cases}$$

$$k = N+m-1, N+m, \ldots, 2N-2$$

where $kk = k-N+2$ and $jj = j-N-3$

$$q_{kj} = \begin{cases} g_{m,j1} & N+3 \leqslant j \leqslant N+m+3 \\ -h_{m+1,j2} & N+m+4 \leqslant j \leqslant 2N+4 \\ 0 & \text{other } j \end{cases}$$

$$k = 2N-1$$

$$q_{kj} = \begin{cases} e_{m+1,j} \exp(\lambda_{aj}) & 1 \leqslant j \leqslant m+1 \\ -f_{N+1,j1} \exp(\lambda_{bj1}) & m+2 \leqslant j \leqslant N+2 \\ 0 & \text{other } j \end{cases}$$

$$k = 2N$$

where $j1 = j-N-2$ and $j2 = j-N-3$

$$q_{kj} = \begin{cases} g_{m+1,j1} & N+3 \leqslant j \leqslant N+m+3 \\ -h_{N+1,j2} & N+m+4 \leqslant j \leqslant 2N+4 \\ 0 & \text{other } j \end{cases}$$

$$k = 2N+1$$

where $j1 = j-N-2$ and $j2 = j-N-3$

$$q_{kj} = \begin{cases} h_{N,jj} & N+m+4 \leqslant j \leqslant 2N+4 \\ 0 & \text{other } j \end{cases} \qquad k = 2N+2$$

where $jj = j-N-3$

$$q_{kj} = \begin{cases} e_{m+1,j} \exp(\lambda_{aj} x_1) & 1 \leqslant j \leqslant m+1 \\ 0 & \text{other } j \end{cases} \qquad k = 2N+3$$

$$q_{kj} = \begin{cases} g_{N+1,jj} \exp(\lambda_{cjj} x_1) & N+3 \leqslant j \leqslant N+m+3 \\ 0 & \text{other } j \end{cases}$$

$$k = 2N+4$$

where $jj = j-N-2$.

Therefore, all constant coefficients can be determined from

$$\mathbf{Z} = \mathbf{Q}^{-1}\mathbf{S} \tag{35}$$

where $\mathbf{Q}^{-1}$ is the inverse of matrix $\mathbf{Q}$.

On finding all coefficients, one has determined the particular solution subject to the determinant conditions given by Tables 1–3, so that intermediate temperatures and the thermal effectiveness P_2 can be readily obtained. Intermediate temperatures in four subregions are given as follows:

$$t_{ai,i+1} = t_{ai}(x=1) = \sum_{j=1}^{m+1} e_j e_{ij} \exp(\lambda_{aj}) \qquad i = 1,3,\ldots,m1$$

$$t_{bi,i+1} = t_{bi}(x=1) = \sum_{j=m+1}^{N+1} f_j f_{ij} \exp(\lambda_{bj}) \qquad i = m+1, m+3,\ldots,N1$$

$$t_{ci,i+1} = t_{ci}(x=0) = \sum_{j=1}^{m+1} g_j g_{ij} \qquad i = 2,4,\ldots,m2$$

$$t_{di,i+1} = t_{di}(x=0) = \sum_{j=m+1}^{N+1} h_j h_{ij} \qquad i = m+2, m+4,\ldots,N2 \tag{36}$$

where

$$m1 = \begin{cases} m-1 & \text{even } m \\ m-2 & \text{odd } m \end{cases} \quad m2 = \begin{cases} m-2 & \text{even } m \\ m-1 & \text{odd } m \end{cases}$$

$$N1 = \begin{cases} N-1 & \text{even } N \\ N-2 & \text{odd } N \end{cases} \quad N2 = \begin{cases} N-2 & \text{even } N \\ N-1 & \text{odd } N. \end{cases}$$

The final dimensionless outlet temperature of the shellside fluid is described by

$$T'' = \frac{T_d(x_2)\dot{W}_c + T_b(x_2)\dot{W}_a}{\dot{W}_1} = \beta_a T_b(x_2) + \beta_c T_d(x_2) = \beta_a \sum_{j=m+1}^{N+1} f_j f_{N+1,j} \exp(\lambda_{bj} x_2) + \beta_c \sum_{j=m+1}^{N+1} h_j h_{N+1,j} \exp(\lambda_{dj} x_2). \tag{37}$$

With the relationship $T'' = 1 - P_1$, one has

$$P_1 = 1 - T'' = 1 = -\beta_a T_b(x_2) - \beta_c T_d(x_2). \tag{38}$$

Therefore, the thermal effectiveness of the $1-N$ split-flow exchanger P_2 is calculated from

$$P_2 = (1 - \beta_a T_b(x_2) - \beta_c T_d(x_2)) R_1. \tag{39}$$

By means of the final dimensionless temperature change of the tubeside fluid, P_2 can be also expressed as

$$P_2 = \begin{cases} t_{c1}(0) = \sum_{j=1}^{m+1} g_j g_{1j} & \text{tubeside flow pattern I} \\ t_{dN}(0) = \sum_{j=m+1}^{N+1} h_j h_{Nj} & \text{tubeside flow pattern II.} \end{cases} \tag{40}$$

Furthermore, the log mean temperature difference correction factor $F = \Delta t_m / \Delta t_{\log}$ for the split-flow exchanger can be determined by

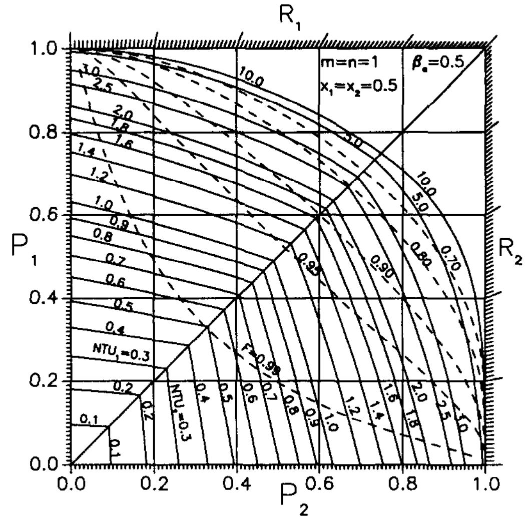

FIG. 2. 1–2 split-flow heat exchanger ($\varepsilon_1 = \varepsilon_2 = 0.5$) with tube flow pattern I.

$$F = \frac{\ln \dfrac{1-P_2}{1-P_2 R_2}}{NTU_2(R_2 - 1)}. \tag{41}$$

So far, we have derived all formulas needed for the thermal calculation of the split-flow exchanger with an even number N of tube passes. The solution for odd N can be readily obtained in the same way.

3. CALCULATION EXAMPLES

Utilizing the previous formulas, we have executed a few calculation examples. The results are plotted in P_1–P_2 diagrams, which show curves with constant NTU and F. Figure 2 gives the thermal performance of a two tube pass split-flow exchanger with tube flow pattern I at the known parameters, such as $\beta_a = 0.5$, $L_1/L = L_2/L = 0.5$ and $\varepsilon_1 = \varepsilon_2 = 0.5$. Figure 3

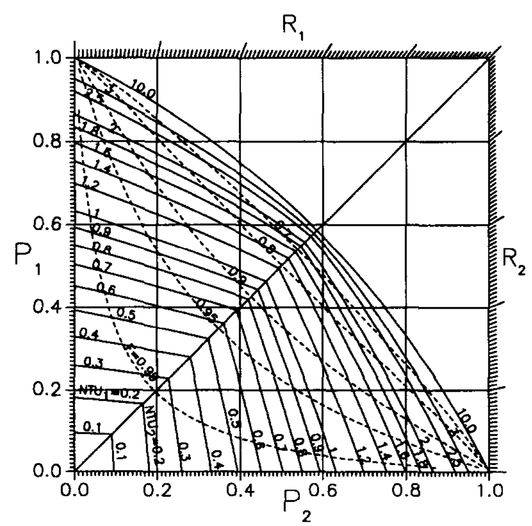

FIG. 3. 1–2 conventional heat exchanger ($\varepsilon_1 = 0.5$, $\varepsilon_2 = 0.5$).

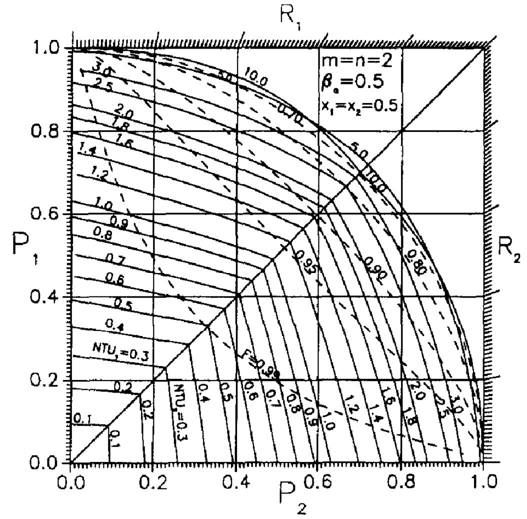

FIG. 4. 1–4 split-flow heat exchanger ($\varepsilon_1 = \varepsilon_2 = \varepsilon_3 = \varepsilon_4 = 0.25$) with tube flow pattern I.

shows the thermal performance of two tube pass conventional exchangers at the known parameters $\varepsilon_1 = \varepsilon_2 = 0.5$. Comparing these two figures, one can realize that the thermal effectiveness P_2 of the split-flow exchanger will increase with NTU and the thermal effectiveness of the conventional exchanger almost ceases to increase with NTU, when $NTU > 3.0$. With the same value of the logarithmic mean temperature difference correction factor F, there are greater values of P_2 for the split-flow exchanger. Figure 2 also illustrates that there is no peak value for the thermal effectiveness P_2 even at greater values of NTU, which is different from the thermal behaviour of the divided-flow exchangers [8]. NTU and F curves for a 1–4 split-flow exchanger are plotted in Figs. 4 and 5. Obviously, the slopes of these curves vary with tube flow patterns.

The thermal performance of the split-flow exchanger with tube flow pattern I is considerably higher than that of the same type of exchangers with tube flow pattern II, because the former can efficiently utilize the temperature difference between the shellside fluid and the tubeside fluid. Therefore, tube flow pattern II should be avoided. It is worth pointing out that the reverse heat transfer may take place in 1–4 split-flow exchangers, when $NTU > 5.0$. This phenomenon is not expected and designers should pay attention to it. Figure 6 shows constant NTU and F curves for a 1–6 split-flow heat exchanger with tube flow pattern I. Comparison among Figs. 2, 4 and 6 reveals that two, four and six tube pass exchangers have nearly identical thermal performance, when $NTU < 4.0$. In design, conventional shell and tube exchangers with even N are usually treated as 1–2 exchangers. Obviously, the same design rule can be applied to split-flow exchangers.

4. PRESSURE DROP

In a heat exchanger with the split-flow pattern, the pressure drop on the shellside will be dominated by the distribution of the shellside fluid. Without consideration of the influence of baffles, this pressure drop can be approximately described as [9]

$$\Delta P_s \sim \frac{\omega^{\alpha} L_x}{d} \tag{42}$$

where

$$\alpha = \begin{cases} 1 & \text{laminar} \\ 1.75 & \text{turbulent} \end{cases}$$

and L_x is the flow length of a pass. Usually, the pressure drop on both shellside flow paths in the split-flow exchanger should be equal to each other, i.e.

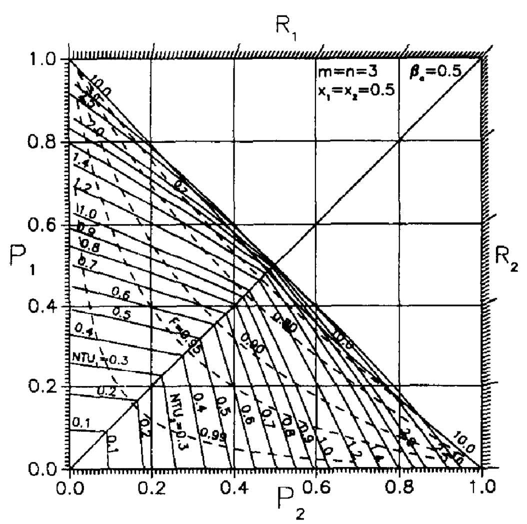

FIG. 5. 1–4 split-flow heat exchanger ($\varepsilon_1 = \varepsilon_2 = \varepsilon_3 = \varepsilon_4 = 0.25$) with tube flow pattern II.

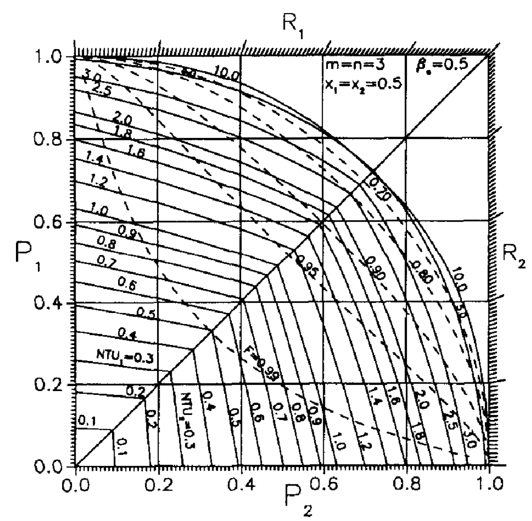

FIG. 6. 1–6 split-flow heat exchanger ($\varepsilon_1 = 0.2$, $\varepsilon_2 = \varepsilon_3 = 0.15$, $\varepsilon_4 = 0.2$, $\varepsilon_5 = \varepsilon_6 = 0.15$) with tube flow pattern I.

$$\Delta P_s = \Delta P_{sa} + \Delta P_{sb} = \Delta P_{sc} + \Delta P_{sd}. \quad (43)$$

If the equivalent transverse diameter of the shell flow tunnel over the longitudinal baffle equals that of the shell flow tunnel below the baffle, one can have

$$\dot{W}_a^\alpha (L - L_1) + \dot{W}_a^\alpha (L - L_2) = \dot{W}_c^\alpha L_1 + \dot{W}_c^\alpha L_2. \quad (44)$$

Rearrangement of equation (44) yields

$$\beta_a = \frac{1}{1 + \left(\frac{2}{x_1 + x_2} - 1\right)^{1/\alpha}} \quad (45)$$

which means that the division of the shellside flow is not arbitrary once the entrance and exit locations of the shellside fluid have been chosen, if equation (43) holds.

In a conventional shell and tube exchanger with N tube passes, the pressure drop on the shellside can be described as

$$\Delta P_s^* = \frac{\sigma \dot{W}_1^\alpha L}{D}. \quad (46)$$

Comparing equation (43) with equation (46), one has

$$\frac{\Delta P_s}{\Delta P_s^*} = \frac{\Delta P_{sa} + \Delta P_{sb}}{\frac{\sigma \dot{W}_1^\alpha L}{D}}. \quad (47)$$

In general, the longitudinal baffle divides the whole transverse flow tunnel of the shellside flow into two equal parts in the split-flow exchanger, so that the equivalent transverse diameter of the tunnels for $\dot{W}_a$ and $\dot{W}_b$ can be expressed as

$$d = \frac{\sqrt{2}}{2} D \quad (48)$$

therefore, equation (47) can be rewritten as

$$\frac{\Delta P_s}{\Delta P_s^*} = \sqrt{2}\beta_a^\alpha (2 - x_1 - x_2). \quad (49)$$

Insertion of equation (45) into equation (49) gives

$$\frac{\Delta P_s}{\Delta P_s^*} = \frac{2\sqrt{2}\beta_a^\alpha (1 - \beta_a)^\alpha}{(1 - \beta_a)^\alpha + \beta_a^\alpha}. \quad (50)$$

Undoubtedly, the right-hand side of equation (49) or (50) is less than 1.0, which signifies that the shellside pressure drop in the split-flow exchanger is smaller than that in the conventional shell and tube exchanger of the equal whole thermal flow rate on the shellside.

In general, the distribution of the shellside fluid will result in the variation of the overall heat transfer coefficient U. To simplify the discussion, we will think about the following two extreme cases:

(1) If the major heat transfer resistance lies on the tubeside, the overall heat transfer coefficient can be considered to be independent of the division of the shellside fluid. In this case the influence of the distribution change of the shellside fluid upon the overall heat transfer coefficient can be neglected and equation (49) or (50) can be directly used to analyse the shellside pressure drop in the split-flow exchangers.

(2) If the heat transfer resistance on the shellside is controlling, the overall heat transfer coefficient is approximately equal to the heat transfer coefficient on the shellside and will vary with the distribution of the shellside fluid. Assuming that the shellside flow is turbulent, one can have the formula to calculate the shellside heat transfer coefficient [10], which approximates the overall heat transfer coefficient

$$U = c_h \omega^{0.6}. \quad (51)$$

In the split-flow exchanger the heat transfer area is divided into subregions a, b, c and d, by means of thermal flow rate, the overall UA can be described as

$$\begin{aligned}(UA) &= (UA)_a + (UA)_b + (UA)_c + (UA)_d \\ &= c_h^*\left(\frac{\dot{W}_a}{d}\right)^{0.6} (L - L_1)\frac{A}{2L} + c_h^*\left(\frac{\dot{W}_a}{d}\right)^{0.6} (L - L_2)\frac{A}{2L} \\ &\quad + c_h^*\left(\frac{\dot{W}_c}{d}\right)^{0.6} L_1 \frac{A}{2L} + c_h^*\left(\frac{\dot{W}_d}{d}\right)^{0.6} L_2 \frac{A}{2L}. \quad (52)\end{aligned}$$

In a conventional shell and tube exchanger with the same value of the shellside thermal flow rate $\dot{W}_1$ and of the overall heat transfer area A as the split-flow exchanger, one has

$$(UA)^* = c_h^*\left(\frac{\dot{W}_1}{D}\right)^{0.6} A. \quad (53)$$

Comparison of equation (52) with equation (53) yields

$$\begin{aligned}\frac{UA}{(UA)^*} = \frac{NTU_1}{NTU_1^*} &= 0.6156(\beta_a^{0.6}(2 - x_1 - x_2) \\ &\quad + (1 - \beta_a)^{0.6}(x_1 + x_2)). \quad (54)\end{aligned}$$

Equation (45) can be inserted in equation (54), if relationship (43) is held. One should combine equation (54) with equation (49) or equation (50) to estimate the merits of the split-flow exchanger, if the heat transfer resistance on the shellside is crucial.

5. OPTIMUM ENTRANCE AND EXIT

It is clear that the thermal effectiveness of the split-flow exchanger varies with the entrance and exit locations of the shellside fluid. We will take a 1–2 split-flow exchanger as an example to discuss the influence of the entrance and exit locations upon the thermal effectiveness. According to the previous procedure, one can readily obtain the formula for calculating the thermal effectiveness of a 1–2 split-flow exchanger with tube flow pattern I at arbitrary entrance and exit locations of the shellside fluid as well as arbitrary β_a

$$P_2 = \rho_1 - \frac{NTU_2}{NTU_1}\beta_c\rho_2 \tag{55}$$

where

$$\rho_1 = 1 - \rho_2 \exp(\lambda_c x_1)$$

$$\rho_2 = \frac{1-r}{r(1-\exp(\lambda_c x_1)) - \dfrac{s+\exp(\lambda_a)-\exp(\lambda_a x_1)}{u}}$$

$$r = \frac{\dfrac{NTU_2}{NTU_1}\beta_c(1-\exp(\lambda_d x_2))}{1+\dfrac{NTU_2}{NTU_1}\beta_c}$$

$$s = \left(\frac{NTU_2}{NTU_1}\beta_a \exp(\lambda_a x_2) - \exp(\lambda_b)\right)\frac{\exp(\lambda_a)}{\exp(\lambda_b)}$$

$$u = \frac{1-\dfrac{NTU_2}{NTU_1}\beta_a}{1+\dfrac{NTU_2}{NTU_1}\beta_c}\,\frac{\exp(\lambda_a x_1)}{\exp(\lambda_c x_1)}$$

$$\lambda_a = NTU_2\varepsilon_1 - \frac{NTU_1}{\beta_a}\varepsilon_1$$

$$\lambda_b = \frac{NTU_1}{\beta_a}\varepsilon_2 - NTU_2\varepsilon_2$$

$$\lambda_c = \frac{NTU_1}{\beta_c}\varepsilon_1 + NTU_2\varepsilon_1$$

$$\lambda_d = -NTU_2\varepsilon_2 - \frac{NTU_1}{\beta_c}\varepsilon_2.$$

It must be emphasized that equation (55) should fail, if $\lambda_a = 0$ or $\lambda_b = 0$. From equation (55), one can determine the optimum entrance and exit locations of the shellside fluid at which thermal effectiveness P_2 will reach the maximum value. To do this, one should take equation (45) as a constraint, if equation (43) is observed.

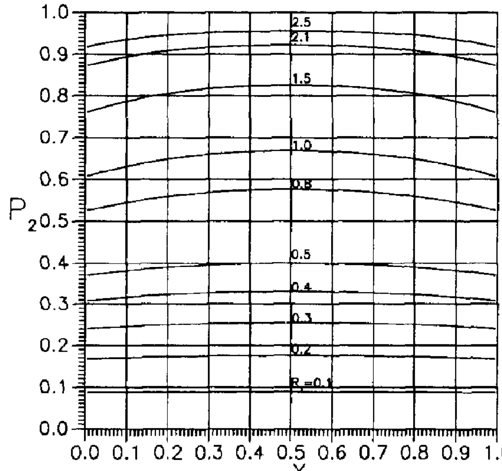

FIG. 8. Thermal effectiveness vs x_1 ($m = n = 1$, $NTU_1 = 2.5$, $x_2 = 1 - x_1$) with tube flow pattern I.

We have carried out some preliminary calculations, considering the following two relationships between the entrance location x_1 and exit x_2, respectively, i.e. $x_2 = 1 - x_1$ or $x_2 = x_1$. The calculation results are plotted in Figs. 7–10, which show that the thermal effectiveness P_2 reaches the maximum at $x_1 = x_2 = 0.5$. In other words, the entrance and exit of the shellside fluid should be located in the middle of the split-flow exchanger to obtain the maximum thermal effectiveness. Figure 10 is made pertinent to the case that the heat transfer resistance on the shellside is a limiting factor. Comparing Fig. 7 with Fig. 9, one can easily find that heat transfer in the split-flow exchanger will greatly degenerate if $x_1 = x_2$, with

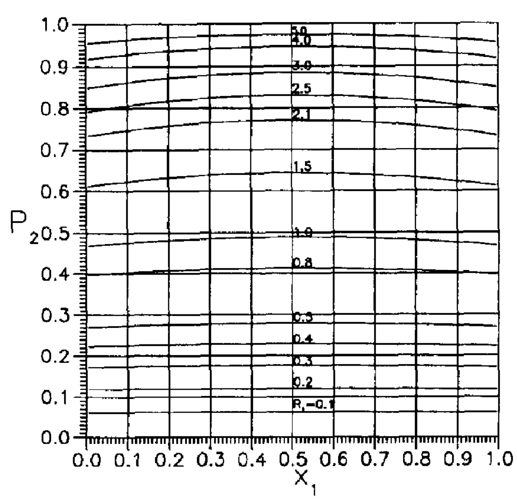

FIG. 7. Thermal effectiveness vs x_1 ($m = n = 1$, $NTU_1 = 1.0$, $x_2 = 1 - x_1$) with tube flow pattern I.

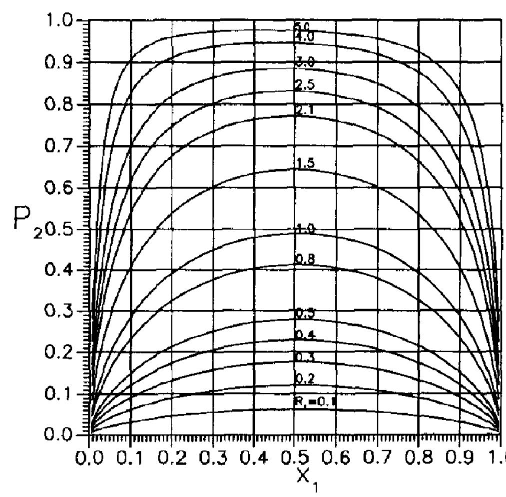

FIG. 9. Thermal effectiveness vs x_1 ($m = n = 1$, $NTU_1 = 1.0$, $x_2 = x_1$) with tube flow pattern I.

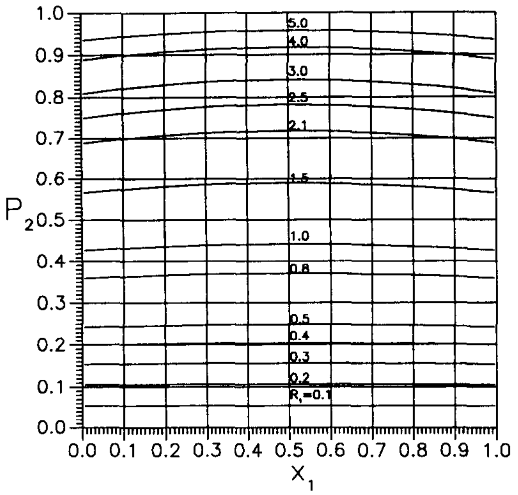

FIG. 10. Thermal effectiveness vs x_1 ($m = n = 1$, $NTU_1^* = 1.0$, $x_2 = 1-x_1$) with tube flow pattern I.

the exception of the point $x_1 = x_2 = 0.5$. With increase of NTU, the influence of the entrance and exit locations of the shellside fluid will become greater, so that designers should pay much attention to the reasonable choice of the parameters x_1 and x_2 to obtain the optimum thermal effectiveness.

6. CONCLUSION

(1) Equations are derived for predicting temperature at a given location on the heat transfer surface and the thermal effectiveness of $1-N$ split-flow exchangers.

(2) For low values of NTU, the thermal performances of split-flow exchangers and of conventional shell and tube exchangers are almost identical, but the split-flow exchanger becomes thermally more efficient as NTU increases. With further augmentation of NTU, the reverse heat transfer may occur in the split-flow exchanger. The shellside pressure drop in the split-flow exchanger is smaller than that in the conventional shell and tube exchanger with the same total thermal flow rate $\dot{W}_1$ and the same length L.

(3) When the entrance and exit of the shellside fluid are located in the middle of the split-flow exchanger, the thermal effectiveness will reach the maximum. With increasing NTU, the influence of the entrance and exit locations upon the thermal effectiveness becomes greater. The arrangement $x_2 = 1-x_1$ is better than the arrangement $x_2 = x_1$ and in the latter case the heat transfer will be deteriorated, except at $x_1 = x_2 = 0.5$.

REFERENCES

1. *Standards of Tubular Exchanger Manufacturers Association* (6th Edn), p. 3. TEMA, New York (1978).
2. D. L. Schindler and H. T. Bates, True temperature difference in a 1–2 divided-flow heat exchanger, *Chem. Engng Prog. Symp. Ser.* **30**(56), 203–206 (1960).
3. K. P. Singh and M. J. Holtz, Generalization of the split flow heat exchanger geometry for enhanced heat transfer, *A.I.Ch.E. Symp. Ser.* **72**(189), 219–226 (1979).
4. K. P. Singh and M. J. Holtz, A comparison of thermal performance of two and four tube pass designs for split flow shells, *J. Heat Transfer* **103**, 169–172 (1981).
5. K. N. Murty, Heat transfer characteristics of one- and two-tube-pass split-flow heat exchangers, *Heat Transfer Engng* **4**(3–4), 26–34 (1983).
6. J. M. Ortega, *Matrix Theory—A Second Course*, p. 29. Plenum Press, New York (1987).
7. Tyn Myint-U, *Ordinary Differential Equations*, p. 132. North-Holland, Amsterdam (1978).
8. Y. Xuan, B. Spang and W. Roetzel, Thermal analysis of shell and tube exchangers with divided-flow pattern, *Int. J. Heat Mass Transfer* **34**, 853–861 (1991).
9. *VDI-Wärmeatlas*, Ll1–Ll10. VDI-Verlag GmbH, Düsseldorf (1984).
10. J. G. Knudsen and D. L. Katz, *Fluid Dynamics and Heat Transfer*, p. 514. McGraw-Hill, New York (1958).

PERFORMANCES THERMIQUES DES ECHANGEURS A ECOULEMENT SEPARE

Résumé—Une analyse est développée pour les échangeurs thermiques à écoulement séparé avec un nombre pair de passes en tube, des positions de l'entrée et de la sortie de l'écoulement dans la calandre, une division arbitraire de l'écoulement et un *NTU* variable. Une solution analytique est présentée pour le calcul de la température et un point quelconque et l'efficacité thermique. La performance thermique de cet échangeur est comparée à celle d'un échangeur conventionnel. La perte de pression du côté de la calandre est discutée ainsi que les emplacements de l'entrée et de la sortie de l'écoulement en calandre dans ce type d'échangeur.

THERMISCHE LEISTUNG VON ROHRBÜNDELWÄRMEÜBERTRAGERN MIT GETEILTEM MANTELSTROM UND LÄNGSUMLENKBLECH

Zusammenfassung—Das thermische Verhalten des Rohrbündelwärmeübertragers mit geteiltem Mantelstrom und Längsumlenkblech wird untersucht. Dabei dürfen mantelseitige Ein- und Austrittsstutzen beliebig liegen und die Aufteilung des Mantelstroms ist variabel. Für die Berechnung der Temperaturprofile und der thermischen Leistung wird eine geschlossene Lösung angegeben. Die thermische Leistung dieses Wärmeübertragertyps wird mit der des normalen Rohrbündelapparates verglichen. Außerdem werden der mantelseitige Druckverlust und die optimale Lage der mantelseitigen Ein- und Austrittsstutzen genauer untersucht.

ТЕПЛОВАЯ ХАРАКТЕРИСТИКА МНОГОХОДОВЫХ ТЕПЛООБМЕННИКОВ

Аннотация—Проводится термический анализ многоходовых теплообменников с четным числом трубных ходов, провизвольным расположением входа и выхода внешнего потока, произвольным его делением и изменяющимися потенциалами переноса. Представлено решение в замкнутой форме для расчета температуры при заданном расположении и к.п.д. Сравниваются тепловые характеристики многоходовых теплообменников и обычного кожухотрубного. Обсуждаются перепады давления в кожухе, а также оптимальное расположение входа и выхода внешнего потока в теплообменнике.